

## Design of time-to-lane-crossing based haptic steering guidance

Oudshoorn, Sjors; Kolekar, Sarvesh; Abbink, David; Petermeijer, Bastiaan

**Publication date**

2018

**Document Version**

Final published version

**Published in**

Proceedings of the Human Factors and Ergonomics Society Europe Chapter 2018 Annual Conference

**Citation (APA)**

Oudshoorn, S., Kolekar, S., Abbink, D., & Petermeijer, B. (2018). Design of time-to-lane-crossing based haptic steering guidance. In D. de Waard, K. Brookhuis, D. Coelho, S. Fairclough, D. Manzey, A. Naumann, L. Onnasch, S. Röttger, A. Toffetti, & R. Wiczorek (Eds.), *Proceedings of the Human Factors and Ergonomics Society Europe Chapter 2018 Annual Conference: Technology for an Ageing Society* (pp. 105-118). Human Factors and Ergonomics Society.

**Important note**

To cite this publication, please use the final published version (if applicable).  
Please check the document version above.

**Copyright**

Other than for strictly personal use, it is not permitted to download, forward or distribute the text or part of it, without the consent of the author(s) and/or copyright holder(s), unless the work is under an open content license such as Creative Commons.

**Takedown policy**

Please contact us and provide details if you believe this document breaches copyrights.  
We will remove access to the work immediately and investigate your claim.

# Design of time-to-lane-crossing based haptic steering guidance

---

*Sjors Oudshoorn, Sarvesh Kolekar, David Abbink, & Sebastiaan Petermeijer  
Department of Cognitive Robotics, Delft University of Technology  
The Netherlands*

## Abstract

Current haptic control systems provide feedback torques based on a lateral deviation with respect to a reference trajectory (i.e., centre of the lane), which do not capture the satisficing behaviour human beings typically adopt during a lane keeping task. As such, a novel time-to-lane-crossing-based controller is proposed, which is expected to provide more human-like guidance. The aim of this study is to describe a novel time-to-lane-crossing-based controller and investigate its potential as an alternative to previous reference-trajectory-based guidance. In a simulator study twenty-four participants drove three trials through a single-lane, 10.8 km long road (width: 3 m), receiving three types of guidance, namely 1) none (manual), 2) reference based controller, 3) TLC-based controller. Results showed that both the reference-based, as well as the TLC-based guidance provided significant safety benefits, in terms of more centred and less varying lane position, and higher safety margins. Moreover, no significant differences were revealed between the two guidance approaches. In conclusion, the TLC-based guidance is a potential alternative to reference trajectory-based guidance. Nevertheless, a more detailed analysis is warranted to investigate the two approaches in different driving conditions, like road width, straights, and curves.

## Introduction

Haptic shared control has been proposed as a viable alternative to complete automation for multiple applications, such as surgery (Li and Okamura, 2003; Nudehi et al., 2005), teleoperation (Sheik-Nainar et al., 2005) and vehicle operation (Griffiths & Gillespie, 2005; Forsyth & Maclean, 2006; Mars et al., 2014). It has been argued that haptic shared control provides performance benefits as well as keeps the operator engaged in the perception-action cycle (Abbink et al., 2018), consequently mitigating many well-known automation issues, like vigilance loss.

For driving, a haptic shared control is usually provided through an actuated steering wheel to assist lateral control (Mulder et al., 2012) or an actuated gas pedal for longitudinal control (Mulder et al., 2011). In lane keeping and curve negotiation tasks, studies have shown haptic shared control yielded benefits in terms of decreased lateral deviation with respect to the lane centre line (Forsyth & Maclean,

In D. de Waard, K. Brookhuis, D. Coelho, S. Fairclough, D. Manzey, A. Naumann, L. Onnasch, S. Röttger, A. Toffetti, and R. Wiczorek (Eds.) (2019). Proceedings of the Human Factors and Ergonomics Society Europe Chapter 2018 Annual Conference. ISSN 2333-4959 (online). Available from <http://hfes-europe.org>

2006; Mohellebi et al., 2009; Saleh et al., 2013; Mulder, et al., 2008) a reduction in workload (Mars et al., 2014; Van Der Horst, 2004) and safety margins (i.e., time-to-lane-crossing; Melman et al., 2017) compared to manual driving. However, haptic shared control has also been reported to increase physical effort (i.e., steering torques).

Increased driver torques have been hypothesized to be the result of conflicts between the driver and the haptic guidance system (Mars, et al., 2014). Conflicts arise when a mismatch occurs between the driver and automation intention. For example, when the driver wants to cut into a curve, but the automation is programmed to drive in the centre of the lane. Indeed, it has been reported in a simulator study that participants had to ‘fight’ the controller (Abbink et al, 2011), which can worsen the overall performance (Griffiths & Gillespie, 2005; Mars, et al., 2014) and decrease acceptance (Petermeijer, et al., 2015). To reduce conflicts, the intention of the automation should match that of the driver closely.

Most of the current haptic steering guidance systems for lane keeping minimize either the lateral deviation and/or the vehicle heading deviation with respect to a reference trajectory (e.g., the centre of the lane, Griffiths & Gillespie, 2005; Mohellebi et al., 2009; Saleh et al., 2013; Abbink & Mulder, 2000). The resulting guidance system operates as an optimizing controller. However, it has been argued that drivers adopt satisficing instead of optimizing behaviour, i.e. is they aim to stay within certain safety thresholds (Goodrich, 2000). Accordingly, Boer (2016) argued that haptic shared control should provide guidance based on safety margins, more specifically based on time-to-lane-crossing (TLC, Van Winsum and Godthelp, 1996).

TLC serves as a measure of situational criticality (Saleh et al., 2013; Van Winsum et al., 2000). It is a metric for lateral control of the vehicle, analogous to time-to-collision in longitudinal control, which has successfully been used to provide guidance forces on a haptic gas pedal (Mulder et al, 2011) and in obstacle avoidance systems (Della Penna et al., 2010). Yet, to the best of our knowledge, no previous efforts have been made to assist drivers in a lane keeping task by a time-to-lane-crossing-based haptic steering system.

TLC is dependent on road curvature, lane width, velocity, vehicle orientation and steering wheel angle, which causes a TLC-based controller to adapt inherently to changing driving conditions, like road width or velocity. Such behavioural changes are similar to those of human drivers as driving conditions change (Van Winsum and Godthelp, 1996).

Although the conceived benefits of TLC-based steering guidance are promising, its use in a control structure, rather than as an evaluation metric, is subject to limitations. TLC is a non-linear parameter, with discontinuities when the lane boundary to be crossed switches (Van Winsum et al., 2000). As the vehicle approaches the lane boundary, small steering corrections can inflate (or deflate) the measured criticality. Moreover, TLC by itself does not have a direction; whilst it offers quantification of criticality, it does not inherently provide a direction towards safety.

In this paper, a control structure is proposed to alleviate the aforementioned limitations of TLC, by means of incorporating human-like uncertainty around the current trajectory, generating a field of safe travel (Boer, 2016). A trigonometric approach for TLC computation is elaborated (Van Winsum et al., 2000), and a driving-simulator study is conducted to evaluate the benefits and limitations of the developed criticality-based haptic steering guidance, in comparison to a previously developed reference trajectory-based guidance system (Mulder et al., 2012).

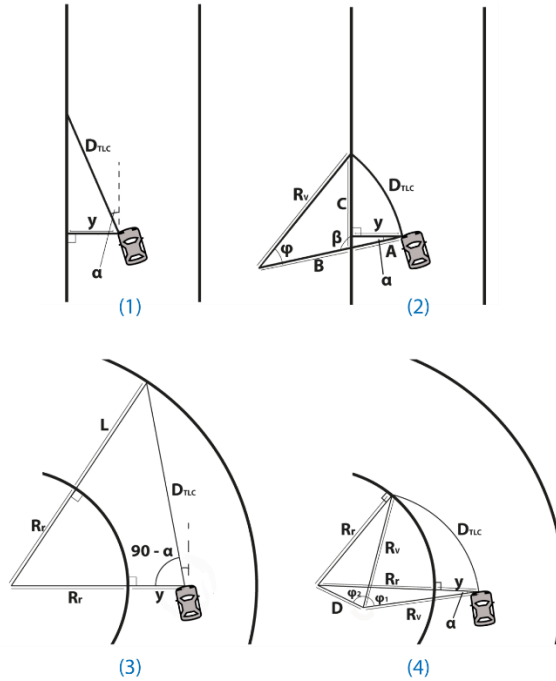


Figure 1. TLC calculation for straight (top) and curved road sections (bottom). Vehicle trajectories are indicated by DTLC and are assumed to have a constant velocity and steering wheel angle. (1) Straight driving on a straight road; (2) Straight road with steering input; (3) Straight driving on a curved road; (4) Driving on a curved road with steering input. Symbols:  $\alpha$ : heading deviation,  $y$ : lane margin,  $R_v$ : vehicle curve radius,  $R_r$ : inner road curve radius,  $L$ : lane width.

### A trigonometric approach to compute TLC

#### Trigonometric TLC computation

In this paper we present an extension of the trigonometric approach of TLC-calculation, based on derivation from Boer (2016) and Van Winsum et al. (2000), which offers an accurate, reliable and robust estimation of the TLC. The trigonometric approach requires consideration of four different scenarios (see Figure 1), namely driving a straight (steering wheel angle = 0) or curved vehicle trajectory (steering wheel angle  $\neq 0$ ), on either a straight or curved road section. The vehicle drives with a velocity  $v$  ( $\text{m}\cdot\text{s}^{-1}$ ); furthermore, steering wheel angle and velocity are

assumed constant. A kinematic bicycle model as in (Rajamani, 2006) was used to describe lateral vehicle motion.

*Straight road, straight trajectory*

The vehicle has a margin to the lane boundary  $y$  (m) from front left or front right wheel, with heading deviation  $\alpha$  (deg) between road and vehicle heading.

$$TLC = \frac{y \cdot \sin(\alpha)}{v} \quad (1)$$

*Straight road, curved trajectory*

When steering input is not equal to zero, the vehicle follows a curved trajectory, with yaw-rate  $\dot{\psi}$  (rad·s<sup>-1</sup>), which determines the vehicle curve radius  $R_v$  (m), as follows.

$$t_{circ} = \frac{2\pi}{\dot{\psi}} \quad (2)$$

$$d_{circ} = t_{circ} \cdot v \quad (3)$$

$$\begin{aligned} R_v &= \frac{d_{circ}}{2\pi} \\ &= \frac{v}{\dot{\psi}} \end{aligned} \quad (4)$$

Referring to figure 1b:

$$A = \frac{y}{\cos(\alpha)} \quad (5)$$

$$B = R_v - A \quad (6)$$

$$\beta = 90 + \alpha \quad (7)$$

In order to compute  $\varphi$  (deg), length  $C$  (m) needs to be determined, by applying the cosine rule for side  $R_v$  (m), as follows.

$$C = \frac{2B \cdot \cos(\beta) \pm \sqrt{(2B \cdot \cos(\beta))^2 - 4(B^2 - R_v^2)}}{2} \quad (8)$$

Applying the cosine rule to solve for  $\varphi$  (deg) and calculate the corresponding arc length  $D_{TLC}$  (m) to determine TLC (s).

$$\varphi = \arccos\left(\frac{B^2 + R_v^2 - C^2}{2B \cdot R_v}\right) \quad (9)$$

$$TLC = \frac{D_{TLC}}{v} \quad (10)$$

#### *Curved road, straight trajectory*

Driving on a curved road with a straight vehicle trajectory is depicted in Figure 1c. The law of cosines is applied to calculate  $D_{TLC}$  (m), similar to Equation 8. Included in the calculation are heading deviation  $\alpha$  (deg), lateral lane margin  $y$  (m), lane width  $L$  (m) and inner curve radius  $R_r$  (m).

$$A = R_r + y \quad (11)$$

$$B = R_r + L \quad (12)$$

$$D_{TLC} = \frac{2A \cos(\beta) \pm \sqrt{(2A \cos(\beta))^2 - 4(A^2 - B^2)}}{2} \quad (13)$$

#### *Curved road, curved trajectory*

The fourth TLC-calculation is a curved trajectory on a curved road, as visualized in Figure 1d. It requires the calculation of  $\varphi_1$  (deg), through means of computing  $\varphi_2$  (deg) and combined angle  $\varphi_{12}$  (deg).

$$\varphi_{12} = \arccos\left(\frac{D^2 + R_v^2 - (R_r + y)^2}{2R_v \cdot D}\right) \quad (14)$$

$$\varphi_2 = \arccos\left(\frac{D^2 + R_v^2 - R_r^2}{2R_v \cdot D}\right) \quad (15)$$

With  $D$  (m) the distance between the center of  $R_r$  (m) and  $R_v$  (m).

$$\varphi_1 = \varphi_{12} - \varphi_2 \quad (16)$$

$$D_{TLC} = \varphi_1 \cdot R_v \quad (17)$$

The considerations of both previous sections are relevant here. Calculation is altered when vehicle trajectory will cross the outer lane boundary: lane width  $L$  (m) is added to road curve radius  $R_r$  (m). If vehicle heading is also oriented towards the outer lane boundary, the following equations are used for  $\varphi_{12}$  (deg) and  $\varphi_2$  (deg).

$$\varphi_{12} = \arccos\left(\frac{D^2 + R_v^2 - (R_r + L)^2}{2R_v \cdot D}\right) \quad (18)$$

$$\varphi_2 = \arccos\left(\frac{D^2 + R_v^2 - (R_r + y)^2}{2R_v \cdot D}\right) \quad (19)$$

## Guidance approaches

### Reference-based guidance

Earlier, Mulder et al., (2012) developed a controller, that used a predicted lateral deviation with respect to a reference trajectory (i.e., the center of the lane). In this paper we will refer to this approach as the reference-based guidance.

The referenced-based guidance (REF) controls for two parameters, predicted lateral deviation  $e_{\text{future,lat}}$  and predicted heading deviation  $e_{\text{future,heading}}$  at lookahead time  $t_{\text{ha}} = 0.7\text{s}$ , assuming a constant vehicle speed and steering wheel angle. Guidance torques  $T_{\text{guidance}}$  (Nm) were calculated using a three gains, namely P, D, and  $K_{\text{pbg}}$ , see equation 20.

$$T_{\text{guidance}} = (e_{\text{future,lat}} \cdot P + e_{\text{future,heading}} \cdot D) \cdot K_{\text{pbg}} \quad (20)$$

Here,  $e_{\text{future,lat}}$  is defined as positive leftwards of lane centerline,  $e_{\text{future,heading}}$  as positive leftwards of zero heading deviation and  $T_{\text{guidance}}$  as positive in rightwards steering corrections (clockwise). Feedback gains were set to  $P = 0.9$ ,  $D = 0.08$  and  $K_{\text{pbg}} = 2$ .

### TLC-based guidance

Time-to-line crossing approaches 0 s at increasingly risky driving situations. Equation 21 is used to generate a usable deviation signal  $\Delta e$ .

$$\Delta e = \frac{TLC \cdot \gamma + \theta}{TLC \cdot \frac{\gamma}{\phi} + 1} \quad (21)$$

Such that,

$$\lim_{TLC \rightarrow \infty} \Delta e = \phi, \quad \lim_{TLC \rightarrow 0} \Delta e = \theta \quad (22)$$

As such,  $\phi$  and  $\theta$  determine lower and upper bounds of criticality, respectively. Finally, is related to relative weighing between these two bounds. The presence of noise (e.g., motor, sensory, or external noise) influences driving behaviour (Kolekar et al., 2016) to illustrate, drivers usually stay away from the edge of the road, regardless of their accuracy in following the road heading. To account for this noise, the impact from potential steering disturbances on safety margins is taken into

account. Similar to Boer (2016), the current vehicle curve radius  $R_v$  is disturbed with a factor  $\lambda$  ( $m^{-1}$ ).

$$R_\lambda = \frac{1}{R_v^{-1} \pm \lambda} \quad (23)$$

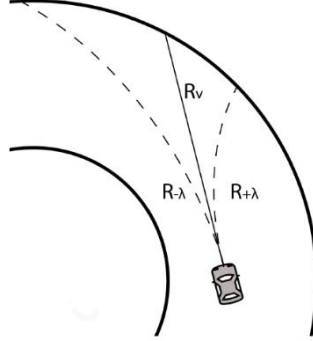


Figure 2. Vehicle trajectory  $R_v$  (steering wheel angle = 0) with left uncertainty boundary  $R_{-\lambda}$  and right uncertainty boundary  $R_{+\lambda}$ .

As shown in Figure 2, driving straight (effectively with  $R_v = \infty$ ) yields two uncertainty trajectories with  $R = \pm \lambda^{-1}$  (m). Conversely, on curved trajectories  $\lambda$  is linearly related vehicle curvature (Boer, 2016). For both uncertainty trajectories, with vehicle curve radius  $R_{-\lambda}$  and  $R_{+\lambda}$  corresponding TLCs are computed. Combining equations 21 and 23 yields equation 24, which is the control algorithm to determine guidance torques  $T_{guidance}$  (Nm), with  $\phi = 0.01$  for lower limit control activity,  $\theta = 10$  for upper limit control activity,  $\gamma = 0.1$  for the relative weighting,  $\lambda = 0.004$  for the driver uncertainty, and  $K_{cbg} = 0.3$  as the deviation-to-torque gain.

$$T_{guidance} = K_{cbg} \left( \frac{TLC_{-\lambda} \cdot \gamma + \theta}{TLC_{-\lambda} \cdot \frac{\gamma}{\phi} + 1} - \frac{TLC_{+\lambda} \cdot \gamma + \theta}{TLC_{+\lambda} \cdot \frac{\gamma}{\phi} + 1} \right) \quad (24)$$

Using this algorithm, driving conditions with equal  $TLC_{-\lambda}$  and  $TLC_{+\lambda}$  will provide zero control input. Figure 3 clearly shows how the TLC-based guidance adapts the feedback torques in relation to road width, compared to the reference-based guidance. Reference-based guidance increases the maximum guidance torque, whereas the TLC-based guidance widens the range of guidance torque; only close to the lane boundary the feedback torques rapidly increase.

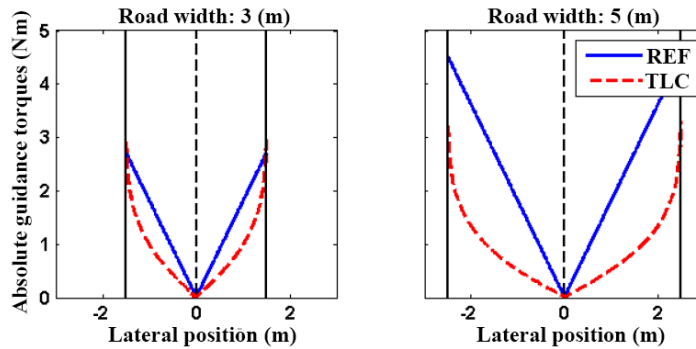


Figure 3. Magnitude of guidance torques, plotted as function of lateral deviation, on a straight road, at velocity  $v = 130$  km/h, heading deviation  $\delta = 0$ , and yaw rate  $\dot{\psi} = 0$ . Performance based guidance (PBG, blue) and criticality-based guidance (red, CBG) are determined for road width = 3 m (left) and road width = 5 m (right).

## Experimental method

### Participants

Twenty-four participants, recruited from the TU Delft student population, took part in the experiment (mean age 24.1, SD 1.9, 16 male). All participants had normal or corrected to normal eyesight, and were in possession of a valid driver's licence for at least one year.

### Apparatus

This study was conducted on a fixed-base simulator; the setup has previously been used (Mulder et al, 2012; Melman et al., 2017; Petermeijer et al., 2015). A dedicated computer controlled a Moog-FCS ECo18000S motor, to provide actuation on the steering wheel at 2500 Hz. The visual environment was updated at 60 Hz; three projectors were used to provide 180 horizontal and 40 vertical field of view.

A single-track model was used for vehicle dynamics to mimic the driving dynamics of a Nissan luxury car (i.e., heavy sedan). An automated gearbox was used, and velocity was fixed at 130 km/h. A light centering stiffness, as a function of the steering wheel angle, was applied in all conditions to emulate wheel-ground interaction forces. Car kinematics, guidance torques, as well as the driver input on the steering wheel were recorded at 100 Hz.

### Road environment

The participants drove the vehicle over a 10.8 km long, single lane road without other traffic, for approximately 5 minutes. The road was composed of straights (length 220 metres), left and right single curves (length 218 metres, inner curve radius 500 metres) and winding sections (four alternations, inner curve radii 500 metres). Curves were interspersed with straight sections (length 150 metres) to prevent crossover effects. Moreover, a long straight section was included to

investigate steady-state behaviour. At the start the vehicle would accelerate to a fixed speed of 130 km/h, until the end of the trajectory, where it would decelerate to zero.

#### *Experimental design and instructions*

Three guidance conditions, namely 1) manual, 2) reference-based guidance (REF), and 3) TLC-based guidance (TLC) were each driven in three trials, namely a training trial, a trial on a normal road (width: 3 m) and a trial on a wide road (width: 5 m). Road width and guidance conditions were counterbalanced over all participants.

All participants read the experiment instructions, signed the informed consent form. Participants were verbally reminded that they are free to pause or stop the experiment at any time (if nausea arises), and to drive as they normally would, and were informed that no other road users would be encountered during the trials. No questions regarding specific controller functionality were answered during the experiment.

After each trial, NASA Task Load Index (NASA-TLX) forms were filled out to assess subjective workload (Hart and Staveland, 1988). Subsequently, participants were inquired for their nausea with a six-item question, ranging from not experiencing any nausea (1) to vomiting (6). The experiment would be stopped if any participant responded with a nausea level of 4 or higher; which did not occur throughout the experiment. After a trial in which steering guidance was presented, participants were interrogated about their acceptance of the assistance system, by means of a five-point scale containing nine items (five related to usefulness, four to satisfaction) (Van Der Laan et al., 1997). After each guidance condition, consisting of three experimental runs of approximately 20 minutes, a five-minute break was taken.

#### *Dependent Measures*

The following dependent measures were analysed for the trials using the normal road width (3 m). Analysis was done on the data recorded between 10 s and 2.5 min of the track.

- Mean absolute lane position (m): a measure of choosing lane position.
- Standard deviation of the lane position (m): a measure that describes the driver's variability in lane keeping performance (i.e., swerving behaviour).
- Median time-to-line crossing (s): a measure of the safety margin throughout the driving task.
- Standard deviation of the steering wheel angle: a measure of the driver's variability of the steering wheel input, which reflects the lane control activity of the driver.

### Statistical analysis

The independent measures were transformed to ranks in order to deal with any non-normal distributions, according to Conover and Iman (1981), before they were subjected to a one-way analysis of variance (ANOVA). A post-hoc analysis was conducted by performing a pairwise comparison using a Tukey honest significance criterion. The significance level was set to 0.05.

### Results

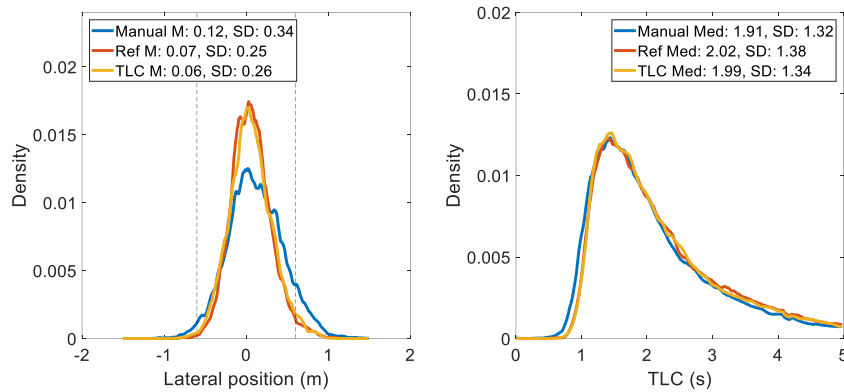


Figure 4. Distribution of the lateral position (left) and time-to-lane crossing (right) per condition. Area underneath the distribution equals one.

Table 1 shows the mean and standard deviations of the independent measures across participants. ANOVAs showed an effect for mean absolute lateral position ( $F(2,69)$

Table 1. Means and standard deviation of vehicle state measures - Straights

Variable	MAN	REF	TLC	ANOVA	Pairwise comparison		
	(1)	(2)	(3)		1-2	1-3	2-3
M abs lateral position (m)	0.282 (0.079)	0.197 (0.066)	0.208 (0.060)	$F(2,69) = 14.24,$ $p < .001$	X	X	
SD lateral position (m)	0.315 (0.076)	0.222 (0.068)	0.246 (0.064)	$F(2,69) = 15.11,$ $p < .001$	X	X	
Median TLC (s)	1.909 (0.103)	2.020 (0.101)	1.991 (0.089)	$F(2,69) = 7.89,$ $p = .001$	X	X	
SD steering wheel angle (deg)	15.830 (1.188)	15.282 (1.033)	15.430 (1.019)	$F(2,69) = 3.41,$ $p = .039$	X		
M abs guidance torque (Nm)	-	0.684 (0.147)	0.685 (0.137)	$F(1,46) = 0.04,$ $p = .839$			

Note: The M abs guidance torques for the manual condition (MAN) are missing, because there are no guidance torques exerted on the steering wheel during manual driving.

= 14.24,  $p < .001$ ), standard deviation of the lateral position  $F(2,69) = 15.11$ ,  $p < .001$ ), the median of the TLC ( $F(2,69) = 7.89$ ,  $p = .001$ ), and the standard deviation of the steering angle ( $F(2,69) = 3.41$ ,  $p = .039$ ). The pairwise comparison revealed that for all metrics except the SD steering wheel angle and the mean guidance torques, the both guidance approaches yielded better performance (i.e., lower mean absolute lateral position, lower standard deviation of the lateral position, and higher median TLCs) from manual driving. For the standard deviation of steering wheel angle only the reference-based guidance was significantly lower than the manual condition. The mean absolute guidance torque did not differ between the reference-based and TLC-based approach.

Figure 4 (left) shows the distribution of the lateral position condition. It can be seen that the manual has a slightly wider distribution compared to the two guidance systems. On the other hand, the two guidance systems seem have the same narrow distribution of lateral position. Meaning, participants drove more in the centre of the lane when they used haptic support.

The right plot in Figure 4 shows the distribution of the time-to-lane crossing per condition. Similar to the left plot it can be seen that the two support systems yield slightly safer behaviour (i.e., higher time-to-lane-crossings) compared to manual driving.

Figure 5 illustrates the mean guidance torques as a function of time-to-lane-crossing. It can be seen that the TLC-based guidance provided lower mean feedback torques compared to reference-based guidance. Note, however, that the TLC-based guidance plot lies more to the left, meaning the TLC-based controller recorded lower time-to-lane-crossings than the reference-based controller.

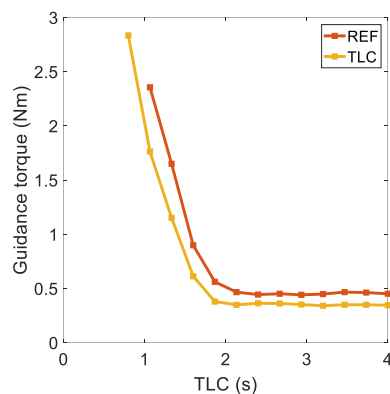


Figure 5. Force feedback as a function of TLC for the two guidance approaches. X-axis: TLC-bins are 0.4 (s) large; Y-axis: The mean guidance torques within the TLC-bin. No TLCs < 0.8 (s) occurred.

## Discussion

Drivers using TLC-based guidance yielded similar behaviour compared to the reference-based guidance, in terms of lateral position and time-to-lane crossing. Note, however, that these metrics were analysed over straight and curved sections of the track with a road width of 3 metres. It was hypothesized that drivers using the TLC-guidance on a wider road will drive more akin to manual drivers (cf. Figure 3). Moreover, it is expected that the two guidance approaches yield different behaviour in the curves, since the TLC-based guidance should allow curve cutting behaviour, whereas the reference-based guidance does not.

In line with the results, the mean guidance torques did not significantly differ between approaches. However, Figure 5 suggests that the guidance torques are quite different for situations with lower values of TLC (i.e.,  $TLC < 1.8$ ). It can be seen that for similar values of TLC the reference-based guidance provides higher torques than the TLC-based ones. These differences are expected to be more distinct for a wider road, since the TLC-based guidance would intrinsically adapt, whereas the reference-based guidance does not.

In the current TLC-based approach, the trigonometric TLC-calculation used four different procedures based on four separate situations (i.e., straight/curved trajectory and straight/curved road). Yet, in future research these calculations can be generalized to one situation, namely the curved trajectory and curved road. The only constraint to this procedure is that a steering angle of exactly zero (i.e., driving straight forward) may never mathematically occur. Though, one can assume a very low steering angle near zero, resulting in a near straight trajectory and similar TLC-values.

## Conclusion

In this study we proposed, developed, and evaluated a novel lane keeping guidance, based on time-to-line-crossing (TLC) in order to mimic a more human-like driver style. In a simulator experiment the novel guidance was compared to manual driving and a previous reference deviation based guidance. Results showed that the two guidance approaches are equally effective in improving lane keeping performance and safety margins compared to manual driving, in terms of absolute lane position and time-to-lane crossing, respectively. Hence, the TLC-based guidance is a viable alternative to the reference-based guidance. Subsequent analysis should be performed to evaluate the approaches separately in curves and straights, and wide roads and narrow ones, since those are sections where more distinct differences are expected to emerge.

## Acknowledgements

D.A. Abbink, S.M. Petermeijer, and S. Kolekar are supported by the Netherlands Organization for Scientific Research (NWO); VIDI project 14127. This paper is a dissemination of the master thesis of Sjors Oudshoorn at the Delft University of Technology. The authors would like to thank Timo Melman for his efforts in supervising Sjors Oudshoorn during this process.

## References

- Abbink, D.A., Carlson, T., Mulder, M., de Winter, J. C., Aminravan, F., Gibo, T.L., & Boer, E.R. (2018). A Topology of Shared Control Systems - Finding Common Ground in Diversity. *IEEE Transactions on Human-Machine Systems*, 99, 1-17.
- Abbink, D.A., & Mulder, M. (2009). Exploring the dimensions of haptic feedback support in manual control. *Journal of Computing and Information Science in Engineering*, 9(1), 011006.
- Abbink, D.A., Mulder, M., & Boer, E.R. (2012). Haptic shared control: smoothly shifting control authority? *Cognition, Technology & Work*, 14(1), 19-28.
- Boer, E.R. (2016). Satisficing Curve Negotiation: Explaining Drivers' Situated Lateral Position Variability. *IFAC-PapersOnLine*, 49(19), 183-188.
- Conover, W.J., Iman, R.L., (1981). Rank transformations as a bridge between parametric and nonparametric statistics. *The American Statistician*, 35, 124-129, <http://dx.doi.org/10.1080/00031305.1981.10479327>.
- Della Penna, M., Van Paassen, M.M., Abbink, D.A., Mulder, M., & Mulder, M. (2010). Reducing steering wheel stiffness is beneficial in supporting evasive maneuvers. In *Systems Man and Cybernetics (SMC), 2010 IEEE International Conference on* (pp. 1628-1635). IEEE.
- Forsyth, B.A.C. and MacLean, K.E. (2006). Predictive haptic guidance: intelligent user assistance for the control of dynamic tasks, *IEEE transactions on visualization and computer graphics*, 12, 103-113.
- Griffiths, P., & Gillespie R. (2004). Shared control between human and machine: haptic display of automation during manual control of vehicle heading. In *Proceedings of the 12th International Symposium on Haptic Interfaces for Virtual Environment and Teleoperator Systems*, pp. 358-366.
- Goodrich, M.A., Stirling, W.C., & Boer, E.R. (2000). Satisficing revisited. *Minds and Machines*, 10, 79-109.
- Kolekar, S.B. (2016). *A Human-like steering model: Based on sensorimotor control theories*. Master's thesis, TU Delft, Delft University of Technology, pp. 1-12.
- Li, M., & Okamura, A. (2003). Recognition of operator motions for real-time assistance using virtual fixtures, *Proceedings of the 11th Symposium on Haptic Interfaces for Virtual Environment and Teleoperator Systems*, pp. 125- 131.
- Mars, F., Deroo, M., and Hoc, J.M. (2014). Analysis of human-machine cooperation when driving with different degrees of haptic shared control, *IEEE transactions on haptics*, 7, 324-333.
- Melman, T., De Winter, J.C.F., & Abbink, D. A. (2017). Does haptic steering guidance instigate speeding? A driving simulator study into causes and remedies. *Accident Analysis & Prevention*, 98, 372-387.
- Mohellebi, H., Kheddar, A., & Espié, S. (2009). Adaptive haptic feedback steering wheel for driving simulators. *IEEE Transactions on vehicular technology*, 58, 1654-1666.
- Mulder, M., Abbink, D.A., & Boer, E.R. (2008). The effect of haptic guidance on curve negotiation behaviour of young, experienced drivers. In *Systems, Man and Cybernetics, 2008. SMC 2008. IEEE International Conference on*, pp. 804-809.

- Mulder, M., Abbink, D.A., & Boer, E.R. (2012). Sharing Control With Haptics: Seamless Driver Support From Manual to Automatic Control, *Human Factors*, 54, 786–798.
- Mulder, M., Abbink, D.A., van Paassen, M.M., & Mulder, M. (2011). Design of a haptic gas pedal for active car-following support. *IEEE Transactions on Intelligent Transportation Systems*, 12, 268-279.
- Nudehi, S., Mukherjee, R., & Ghodoussi, M. (2005). A shared-control approach to haptic interface design for minimally invasive telesurgical training, *IEEE Transactions on Control Systems Technology*, vol. 13, 588–592.
- Petermeijer, S.M., Abbink, D.A., & De Winter, J.C.F. (2015). Should drivers be operating within an automation-free bandwidth? Evaluating haptic steering support systems with different levels of authority. *Human Factors*, 57, 5-20.
- Rajamani, R. (2011). *Vehicle dynamics and control*. Springer Science & Business Media.
- Sheik-Nainar, M.A., Kaber, D.B., and Chow, M.Y., (2005). Control Gain Adaptation in Virtual Reality Mediated Human–Telerobot Interaction, *Human Factors and Ergonomics in Manufacturing*, 15, 259–274.
- Saleh, L., Chevrel, P., Claveau, F., Lafay, J.F., & Mars, F. (2013). Shared steering control between a driver and an automation: Stability in the presence of driver behaviour uncertainty. *IEEE Transactions on Intelligent Transportation Systems*, 14, 974-983.
- Van der Horst, R. (2004). Occlusion as a measure for visual workload: an overview of TNO occlusion research in car driving. *Applied Ergonomics*, 35, 189-196.
- Van Winsum, W., & Godthelp, H. (1996). Speed choice and steering behaviour in curve driving. *Human Factors*, 38, 434-441.
- Van Winsum, W., Brookhuis, K.A., & De Waard, D. (2000). A comparison of different ways to approximate time-to-line crossing (TLC) during car driving. *Accident Analysis & Prevention*, 32, 47-56.